King Saud University

Arabian Journal of Chemistry

www.ksu.edu.sa
www.sciencedirect.com

ORIGINAL ARTICLE

Application of stress induces ascorbate peroxidases of *S. polyrhiza* for green-synthesis Cu nanoparticles

Vipul R. Patel *, Nikhil Bhatt *

Department of Microbiology, Gujarat Vidyapeeth, SADRA, 382320 Dist: Gandhinagar, Gujarat, India

Abstract The objective of this study was to assess the effects of stress on physiology/biochemical component of *S. polyrhiza* and its impact on CuNPs synthesis and bioethanol production. NaCl with RV5 provokes oxidative stress in *S. polyrhiza* and significantly increase MAD, Proline, H_2O_2, ROS, SOD and APX activity compare to control condition. Starch accumulation in *S. polyrhiza* was found 354% higher and correspond 4.4 times higher ethanol yield under stress condition compare to control. CuNPs were synthesized with an average size of 23–26 nm by purified fraction of APX having 37 KDa MW, 1.44 IU specific activity. Synthesized CuNPs were stable up to 15 consecutive cycles and potency against wide range of reactive dyes. The maximum remedial efficiency of synthesized CuNPs for COD and BOD was 55263.3 ± 3298.5 mg/m^{3}min. and 30560.3 ± 1987.5 mg/m^{3}min. respectively for RV5 wastewater. 0.072 mg/g of bioethanol was produced from the wet pulp remaining after nanoparticles synthesis. High efficiency of CuNPs and significant production of Ethanol, indicate that the feasibility for circular model for continuous industrial wastewater treatment.

1. Introduction

More than 70% of the world population currently facing water scarcity issues and the population of the world will reach to 9 billion by 2050, create more critical condition for water and energy (WWAP-UNESCO, 2017). So need to focus on wastewater treatment based circular model for energy generation because at present over 80% of sewage and industrial wastewater as it is discharged due to lack of eco-sustainable treatment deteriorate the quality of surface water and accelerate the eutrophication of coastal marine ecosystems (Verma and Suthar, 2014). On the other side commercial biofuels production based on 1G crops strained the food supplies and 2G feedstock is not economical and has technical challenges. In view of the inherent problems attention has been turned to focus on easily available source which can solved both the propose of economical production of biofuels and will be helpful for the wastewater treatment technology (Rajkumar et al., 2014). Recently several physio-chemical, biological and advance oxidation wastewater treatment processes have been

* Corresponding authors at: Department of Microbiology, Gujarat Vidyapeeth, SADRA, 382320 Dist: Gandhinagar, Gujarat, India.
E-mail addresses: vipul123.brc@gmail.com (V.R. Patel), bhattnikhil2114@gmail.com (N. Bhatt).
Peer review under responsibility of King Saud University.

Production and hosting by Elsevier

designed to improve wastewater quality. But, due to high treatment cost and generating large amount of sludge there is need of cost-effective and scalable alternative wastewater treatment technology that has a low environmental impact, which makes it feasible for large-scale application.

Spirodela polyrhiza is one of the abundant aquatic weed species, attracted recent attention due to world-wide availability and huge amounts of money is spent for removal without making good use of it. Rapid growth, sink large amount of carbon dioxide for their growth, easy to utilized for biofuels production and able to produce industrially important enzymes drawn more attention towards its utilization for welfare of mankind. Recent reports showed that in the environmental stress condition *S. polyrhiza* accumulate high antioxidative enzymes content and high percentage of starch (Geng et al., 2018). Environmental stress triggers the production of abscisic acid and hormones in the plant that closes stomata results in reduction in photosynthesis (Chaves et al. 2009). It also triggers the production H_2O_2, $O^{2\cdot-}$ and $\cdot OH$ led oxidative damage of nucleic acid, proteins and lipids (Potters et al. 2010). For the survival under stress condition plant trigger the activity of Super Oxide Dismutase, Ascorbate peroxidase, Catalases and Glutamate Reductases, important oxidative enzymes for scavenging ROS to H_2O_2 and detoxification of H_2O_2 (Sumithra et al. 2006). Many author had reported the triggering of the antioxidative enzymes especially peroxidases due to the environmental stress (Singh et al., 2018; Geng et al., 2018). To our best knowledge, there is no study representing the use of ascorbate peroxidases of *S. polyrhiza* for the synthesis of CuNPs. economical and hazard-free method of disposing this weed. We report the first the economical and hazard free method for disposing weeds and synthesis of CuNPs using the purified ascorbate peroxidases as reducing and stabilizing agent.

In addition, *S. polyrhiza* system can effectively accumulate up to 64.9% DW under stress condition (Xu et al., 2011). Important feature of *S. polyrhiza* has low fiber and lignin content compared with other plants makes it feasible as feedstock for bioethanol production (Guo et al., 2017). Previous study reported the ethanol yield could 24.1–30.8 g L^{-1} achieved from duckweed biomass (Chen et al., 2012). Considering both the points, *S. polyrhiza* has potential for wastewater treatment and energy generation.

The aim of this study was to find out the response of *S. polyrhiza* upon exposure to NaCl, RV5 and NaCl combine with RV5 with reference to variations in contents of pigment, MDA, proline, ROS, H_2O_2 and APX & SOD activity. Furthermore, the bioethanol production from accumulated starch contents during the stress condition was also considered. It was also examined the efficiency of the CuNPs for wastewater treatment synthesized by the purified APX extracted from *S. polyrhiza*.

2. Materials and methods

2.1. Sample collection and growth condition

S. polyrhiza was collected from a local pond of Charada (23°29′03.89″N and 72°38′49.18″E) Gujarat, India. Dry weight and wet weight of *S. polyrhiza* is mentioned in Supplementary Table 1. After sterilization with 1% NaOCl for 5s, stock cul-

ture was maintained in Schenk-Hildebrandt growth medium at pH 5.6 with 12/12 h light/dark cycle in the 50 mmol $m^{-2}s^{-1}$ irradiance. Plants were subculture at 2 week intervals. Precultivation was developed ten days before experiments in SH growth medium. Experimental procedure was started by inoculating 3–4 fronds/m^2 in small artificial pond with dimensions $100 \times 100 \times 10$ cm^3 containing sewage wastewater in the environmental condition. The plants were exposed to 25–200 mM NaCl, 25–200 ppm RV5 and 25–200 ppm NaCl + RV5 for determination of enzyme activities, proline, MDA, pigments and starch contents after 96 h exposure. All experiments were repeated at least 3 times. Plant growth inhibition was estimated according to following formula,

$$\text{Growth inhibition } (\%) = (1 - \text{the fresh weight of plant} / \text{the fresh weight of control}) \times 100$$

(1)

2.2. Enzyme extraction and assay

0.2 g biomass of *S. polyrhiza* was homogenized in mortar and pestle with liquid N_2. Then the biomass was suspended in 0.8 ml 50 mM potassium phosphate buffer (pH-7.0) having 1 mM EDTA and 1 mM phenyl methyl sulfonyl fluoride. The homogenate was centrifuged at 15,000g for 30 min. at 4 °C and the supernatant was stored at 4 °C temperature for further enzyme assay. The APX activity was determined by monitoring the decomposition of ascorbic acid absorbance at 290 nm (Nakano and Asada,1981). The SOD activity was assayed by monitoring inhibition of photochemical reduction of NBT (Beauchamp and Fridovich,1971). Hydrogen peroxide content was measured (Sumithra et al. (2006). The $O^{2\cdot-}$ was assayed by measuring the reduction of exogenously NBT (Doke 1983).

2.3. Purification of APX

Crude extract of *S. Polyrhiza* was precipitated with $(NH_4)_2SO_4$ at 40–70% of saturation. The precipitates were then collected by centrifugation at 17,000g for 20 min and suspended in 100 ml 25 mM Tris at pH 7.8. The dialysis of the precipitate was carried out overnight against 1L of same buffer. Further the ion exchange chromatography was performed in 2.5 × 23 cm column of DEAE cellulose. Purified enzyme was subjected to non-denaturing, discontinuous mini-gel electrophoresis (Davis 1964). The gel was rinsed and washed with phosphate buffer (pH-7.0), followed by stained in 1 mM 3,3-diaminobenzidine and 0.03% H_2O_2 for detecting the APX activity (Abdelbasset et al. 1995).

2.4. Preparation and characterization of CuNPs

Copper nanoparticles were synthesized by mixing 0.07 mg of purified AOX having 0.1U activity with 0.1 M $CuSO_4 \cdot 5H_2O$ solution in 1:3 ratios. The samples were taken at regular interval for measuring the spectrum over the wavelength range of 200–800 nm till 24 h. The synthesized CuNPs were characterized using DLS, SEM-EDX, XRD and FTIR techniques. All the samples were washed with the ethanol for removing the NaCl contents before XRD analysis. XRD was analyzed in

Philips X'Pert Pro instrument with source of radiation was Cu-K ($Λ$ = 1.54A). Samples were scanned within the 2Θ range from 20 to 70°. CuNPs were sprinkled on adhesive carbon tapes supported on metallic plate, the images and elemental contents were recorded at different magnification by Philips XL-30S FEG type instrument. Functional groups present on the surface of the CuNPs were determine by the FTIR. Spectra was scanned in the range of 4000–400 cm^{-1} using Varian Carry 50 spectrophotometer with 32 times scan and given one reflection that is equal to 21 resolutions.

2.5. Decolorization experiments

Photocatalytic degradation of different reactive dyes was carried out in aqueous medium to evaluate the efficiency of CuNPs. Rectangular borosilicate glass photoreactor having a dimension of 23 × 23 × 18 cm^3 was used for the experiments. A total 400 mg of CuNPs were added per 100 ml of the dye solution. The experiment was started after the addition of the 0.2 ml 30% H_2O_2 per 100 ml in the reaction mixture. The samples were withdrawn and analyzed after every 15 min. for the determination of change in absorbance at $Λ$max of dyes. Hach DR 2010 spectrophotometer and Hatch COD reactor was used for the COD analysis. Percentage of decolorization and rate of decolorization was calculated according to Patel et al. (2013).

$$Decolorization(\%) : \ AC - AT/AC × 100 \qquad (2)$$

Where AC is the absorbance of the control and AT is the average absorbance of test samples.

2.6. Enzymatic hydrolysis of starch for bioethanol production

Biomass slurry remain after CuNPs synthesis, mix with 80% ethanol at 70 °C for 15 min for starch extraction. Further the biomass was heated at 100 °C for 10 min and hydrolyzed by optimized process with α-amyloglucosidase Sigma A7095

and α-amylase Sigma A4582. A 0.5 g of extracted starch was mixed with 1%, 2% and 5% v/v amylases in fix volume (30 ml) of sodium acetate buffer (pH 4.8), incubated at 37 °C for 4 h on an orbital shaker and centrifuged for 5 min. at 12,000*g*. The concentration of glucose was analyzed by water HPLC system equipped with C18 column and Uv–Vis detector. The starch content was determined by following equation;

$$Starch \ content = glucose \ content × 0.909 \qquad (3)$$

Saccharomyces cerevisiae MTCC180 was enriched with peptone (5 g/L) and yeast extract (3 g/L) and used for the fermentation of glucose to ethanol. The fresh yeast culture having 200 CFU/mL was inoculated in the fermentation broth at 28 ± 2 °C on orbital shaker at 180 rpm for 48 h. Samples were withdrawn after 12 h interval for analyzed ethanol yield and re were withdrawn at 12 h interval for analysis of ethanol generated and remaining residual reducing sugar by GC–MS and HPLC method, respectively.

3. Results and discussions

3.1. *S. polyrhiza* growth and nutrient removal from sewage

S. polyrhiza was grown in the sewage keeping the facts in the mind that India is generating above 62,000 MLD sewage and discharging in the environment as it is containing high concentration of nitrogen and phosphorus resulting eutrophic condition in receiving water bodies. The sewage containing TN-46.7 ± 4.2 mg/L, TP-18.3 ± 2.3 mg/L and other contaminants as shown in Table 1. The concentration Ammonia, Nitrate, Nitrite was significantly higher in sewage as 20.4 ± 1.9 mg/L, 19.6 ± 1.6 mg/L and 4.9 ± 0.7 mg/L respectively. After 15 days' experiment, the reduction in concentration of TN, and TP were 89.51% and 95.16% respectively (Table 1). NH_4^+–N concentration gradually decreased during the initial days of the incubation from 20.4 ± 1.9 to 2.4 ± 0.19 mg/l, on the other hand Nitrate and Nitrite concentration was increase by 52.04% and 91.84% respectively. it might be due to dominance of nitrifying bacteria (Ammonia to Nitrate to Nitrite) over denitrifying bacteria (Nitrate to Nitrite to Nitrogen gas) in the rhizosphere of *S. polyrhiza*. The rate of the biomass generation of *S. polyrhiza* was 21.6 ± 1.63 g/m^{2}d. The computational yield of 3.25 ton of fresh biomass after 15 days' incubation by treating 1 MLD of sewage was achieved.

3.2. Effect of exogenous exposure of NaCl and RV5 on macromolecules of *S. polyrhiza*

It was observed that NaCl and RV5 stress significantly reduce the chlorophyll and carotenoids concentration and growth inhibition of S. *polyrhiza* (Supplementary Figs. 1, 2). Stress induced *S. polyrhiza* fronds were analyzed for H_2O_2, ROS, MDA and proline assay. H_2O_2 and ROS content increased significantly as compared to the control plants. The accumulation of H_2O_2 and ROS were 2.34 ± 0.41 and 2.58 ± 0.57 μmol/g FW respectively, which is 5750 and 3585% higher compare to control, 387 and 529% higher compare to only NaCl treatment and 317 and 396% higher compare to only RV5 treatment respectively (Fig. 1a). An increase in H_2O_2 and ROS

Table 1 Physio-chemical characterization of sewage wastewater.

Sr. No.	Parameters	Before treatment	After treatment
1	COD (mg/L)	598.6 ± 21.7	104.3 ± 6.7
2	BOD5(mg/L)	408.7 ± 13.1	84.6 ± 3.5
3	TKN(mg/L)	46.7 ± 4.2	4.9 ± 0.5
4	NH_4^+-N (mg/L)	20.4 ± 1.9	2.4 ± 0.19
5	NO_3^--N (mg/L)	19.6 ± 1.6	1.9 ± 0.16
6	NO_2^--N(mg/L)	4.9 ± 0.7	0.5 ± 0.11
7	TP (mg/L)	18.3 ± 2.3	0.6 ± 0.2
8	TSS (mg/L)	214.5 ± 4.8	22.6 ± 3.4
9	Alkalinity (ppm CaCO₃)	318.7 ± 8.3	81.3 ± 5.7
10	Oil & grease (mg/L)	114.9 ± 2.8	18.3 ± 3.8
11	pH	7.3 ± 0.2	7.1 ± 0.3
12	Phenol (mg/L)	0.84 ± 0.15	0.12 ± 0.08
13	Chloride (mg/L)	118.6 ± 5.4	22.3 ± 5.6
14	Sulphate (mg/L)	3.45 ± 0.7	0.45 ± 0.06
15	Turbidity (NTU)	128 ± 8	8 ± 1
16	Detergent(mg/L)	3.87 ± 0.8	0.47 ± 0.08

content trigger higher lipid peroxidation of polyunsaturated fatty resulted in increase the MDA concentration. Maximum concentration of MDA was 2.56 ± 0.1 nmol/mg protein found at 150 ppm combine exposure of RV5 + NaCl, which was 526% higher compare to control, 164% higher compare to only NaCl exposure and 62% higher compare to only RV5 exposure (Fig. 1b). Further increasing in the concentration up to 200 ppm, decrease the MDA concentration by 84%. In the present study, a dose-dependent increase in MDA concentration compare to control was also found, which indicated that NaCl and RV5 stress damages membrane systems, resulted in cellular integrity loss in *S. polyrhiza*. Previous research also supports the peroxidative damages caused by exogenous hormones in plant and microbes (Belhaj et al., 2017). Accumulation of proline in stress condition is common characteristic of monocot plants and metal stressed common duckweed but not found in giant duckweed. As shown in Fig. 1b the proline was not significantly accumulated compare to control plants. Such phenomena were observed by several researchers, might be due to the accumulation of more proline was found in water deficit plant compare to salt-stressed cells (Ashraf and Harris, 2004). Yamaya and Matsumoto (1989) had observed same results for barley plants. In other words, duckweed have enzymatic complexes or non-enzymatic antioxidants for osmotic adjustment through the under NaCl or RV5 stress (Ashraf and Harris, 2004).

Proline accumulation was not significantly increase but APX and SOD enzymes activity was significantly increase under NaCl and RV5 stress condition and maintain the osmotic balance in the duckweed. The maximum concentration of APX activity was 741.8 ± 65.36 Unit mg^{-1} protein observed at 150 ppm concentration of NaCl + RV5, which is 333% higher compare to control, 67% higher compare to only NaCl treatment and 31% higher compare to only RV5 treatment. Further increasing in the concentration up to 200 ppm decrease the proline concentration was decrease by 71% (Fig. 1c). The maximum concentration of SOD activity was 345.8 ± 61.64 Unit mg^{-1} protein observed at 150 ppm concentration of NaCl + RV5, which is 275% higher compare to control, 175% higher compare to only NaCl treatment and 55% higher compare to only RV5 treatment. Further increasing in the concentration up to 200 ppm decrease the SOD activity by 70% indicating an antioxidative response in plants (Fig. 1c). Higher activity of SOD enzyme indicates the presence of reactive oxygen species in plants exposed to salt or other organic toxicants. APX & SOD have play vital roles during abiotic and biotic stress for growth, respiration, transpiration and gas exchange in plants (Gill and Tuteja, 2010; Doğanlar and Atmaca, 2011). SOD play important roles in neutralizing ROS toxicity by converting O^{2-} to H_2O_2, sequentially POD reduce H_2O_2 into H_2O and O_2 (Ruiz-Lozano and Aroca, 2010). Result shown in Fig. 1a–c, indicate that the *S.*
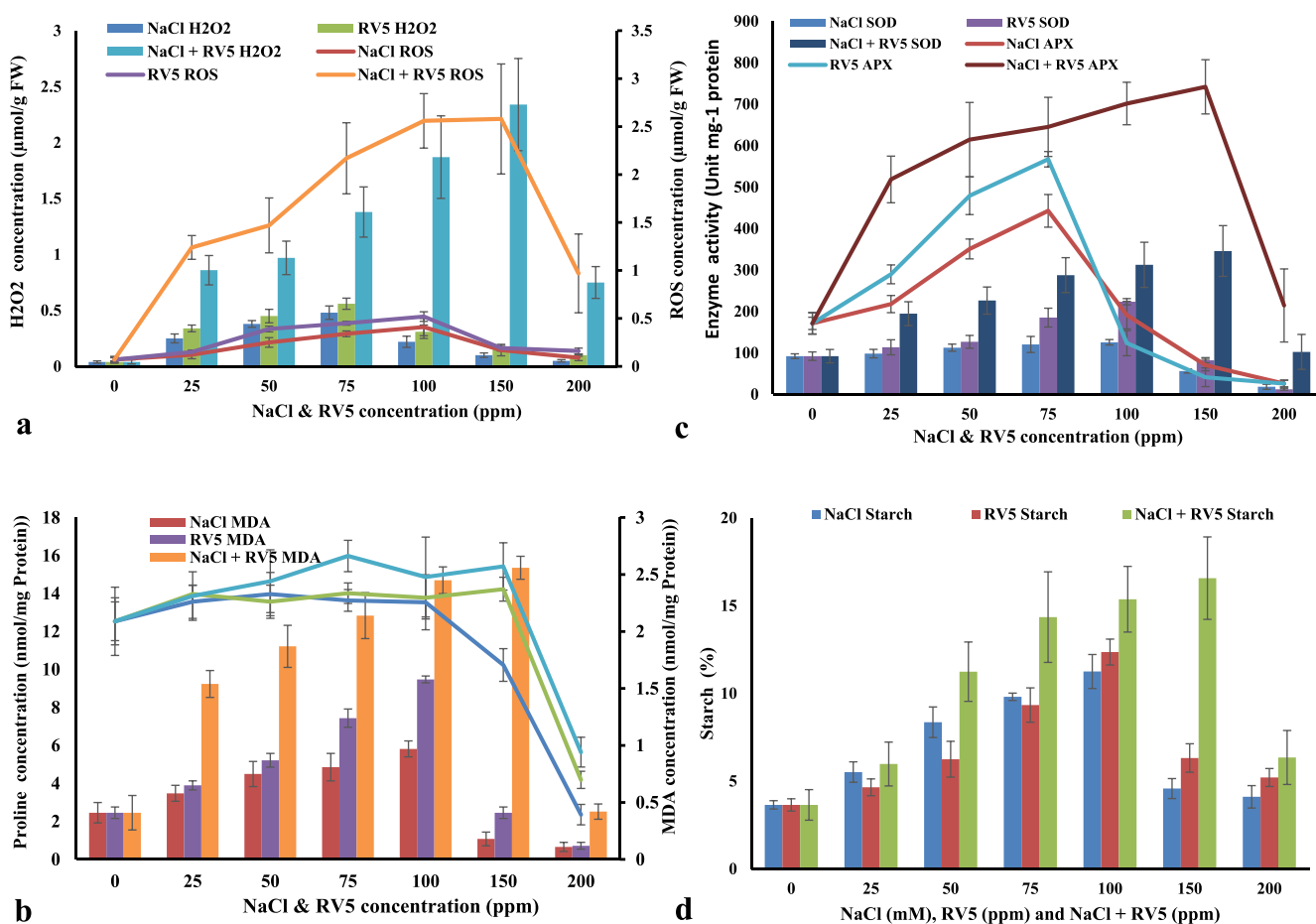
Fig. 1 Effects of different concentrations of NaCl, RV5 and NaCl combine with RV5 on Reactive Oxygen species and H2O2 (a), Proline and MDA (b), APX and SOD enzyme activities (c) and Accumulation of the starch (d) in Spirodela polyrhiza.
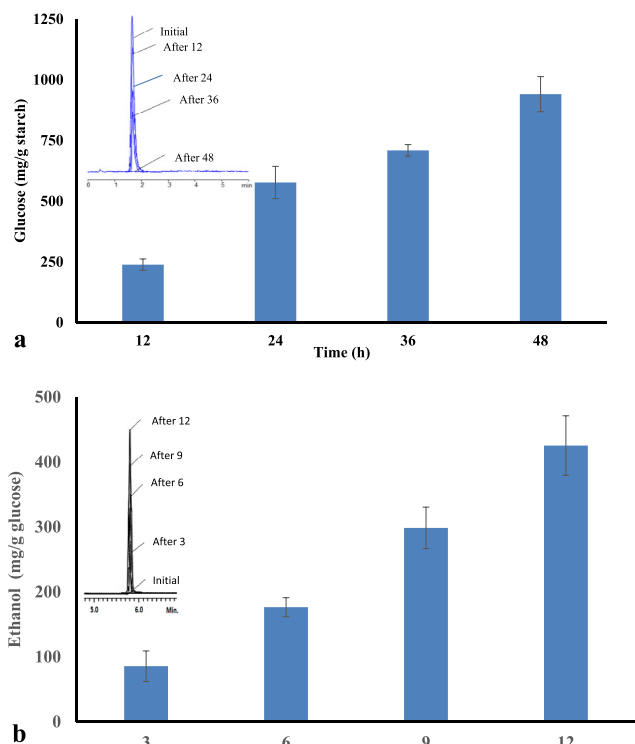
Fig. 2 HPLC analysis of hydrolysates (a), GC–MS analysis at different time interval of fermented broth (a).

polyrhiza tolerated larger oxidative stress by exposed to higher NaCl and RV5 concentrations, which could explain by dose-dependent increase in the concentration of H_2O_2, MDA, ROS, SOD and APX activity. Similar results were also obtained for SOD and APX activity in duckweed exposed to both organic and inorganic pollutants, *C. demersum* (under Pb and Zn stress), *L. minor* (exposed to Cd, Pb and electroporating wastewater) (Torbati et al., 2015, Mishra et al., 2006, Singh and Singh, 2006).

Starch was accumulated $11.25 \pm 0.97\%$ and $12.36 \pm 0.74\%$ in biomass exposed with 100 mM NaCl and 100 ppm RV5 respectively.

But as shown in Fig. 1d the maximum concentration of starch $16.57 \pm 2.35\%$ was achieved from biomass exposed with 150 ppm concentration of NaCl + RV5. It is 354% higher compare to control, 47% higher compare to only NaCl treatment and 34% higher compare to only RV5 treatment. It might be due to some stress factors in stress condition *S. polyrhiza* suppress the vegetative growth and utilize non-utilized photosynthetic molecular carbohydrate in form of the accumulated starch (Sree and Appenroth 2014, Appenroth et al., 2010). Further increasing in the concentration up to 200 ppm decrease the starch accumulation by 62%, might be due to the antioxidative response in plants.

Wet pulp remaining after nanoparticles synthesis containing $16.57 \pm 2.35\%$ Starch and $0.73 \pm 0.05\%$ cellulose. The fractionation or traceable process minimizes 59 to 66% of the chemical use and reduce environmental damage by eliminating defatting treatments compare to conventional starch extraction. Starch was hydrolyzed by α-amyloglucosidase Sigma A7095 and α-amylase Sigma A4582 with 2% optimized dosage, 48 h of hydrolysis period and 45 °C temperature. The hydrolysate was analyzed by HPLC, confirmed formation of glucose 941.21 ± 72.36 mg/g starch, which corresponds to 94.28 ± 1.25 conversion efficiency (Fig. 2a). Fermentation of hydrolysates with *S. cerevisiae* MTCC 180 for 12 h produce ethanol 425.23 ± 45.84 mg/g glucose, which correspond to $87.24 \pm 1.24\%$ conversion efficiency (Fig. 2b and Supplementary Fig. 3). The conversion efficiency of duckweed sugars to ethanol remained between 87 and 89% which is 4.82 to 11.25% higher than those reported for algae using an engineered microbial platform.

Effect of cell free extract of *S. polyrhiza* after treating with different concentration of NaCl + RV5 on size and zeta potential of nanoparticle was one of the major finding of the study. Result shown in the Fig. 3 significant decreasing in size of nanoparticle synthesized and smallest size 21.35 ± 11.23 nm
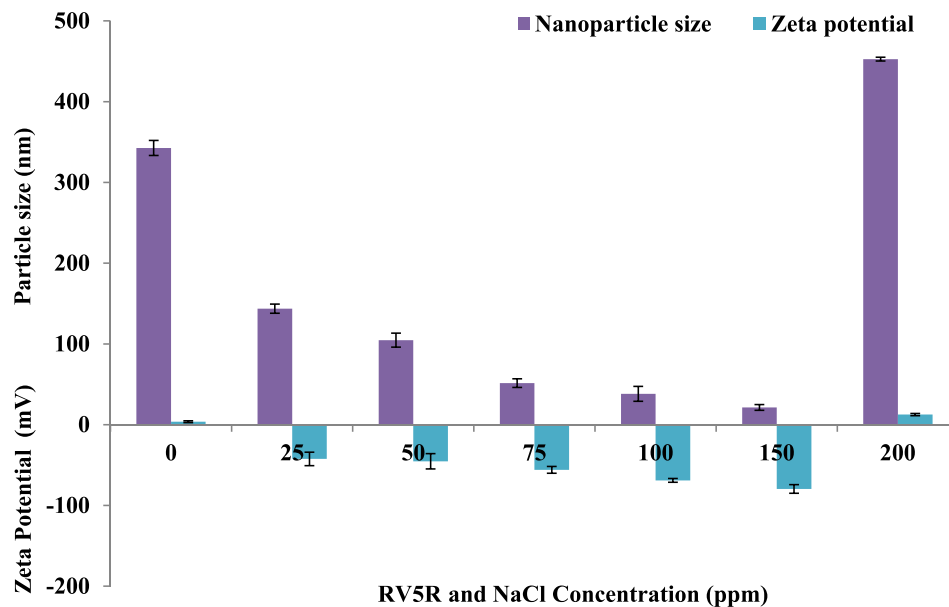
Fig. 3 Effects of cell extract of *S. polyrhiza* treated with different concentrations of NaCl combine with RV5 on size of nano particles and the Zeta potentials.

of CuNPs were achieved at 150 ppm NaCl + RV5, 16-fold reduction in the size compare to control. While further increasing in the concentration NaCl + RV5 up to 200 ppm, 22-fold increase the size of CuNPs. It might be due to duckweed exposed to oxidative stress greater increase of SOD/POD activity play key role for the synthesis for CuNPs. Synthesized silver nanoparticle using lignin peroxidase of the Acinetobacter sp. (Singh et al., 2017). Zeta potential is defining stability and balance between the repulsive and attractive forces of nano-particles. The magnitude of zeta potential directs the electrostatic repulsion between two similar charged particles. So the colloids of nano-particles with high positive or negative zeta potential are electrically more stable. Results of zeta potential was -79.54 ± -5.69 mV at room temperature, confirm the CuNPs is highly stable (Fig. 3).

3.3. Synthesis of nanoparticle and characterization

The cell free extract with 0.226 Umg^{-1} specific activity of APX was used as crude enzyme for the partial purification by $(NH_4)_2.SO_4$ precipitate. The crude enzyme was maximum precipitate at 55% saturation with 2.4-fold purification. The fraction of the best yield was loaded on DEAE-Sephadex, G-200-Sephadex, CM-Sephadex column, G-200-Sephadex, Ammonium sulphate 35% and crystallization sequentially yielding 6.35-fold purification with 1.44 Umg-1 specific enzyme activity (Table 2). Single band correspond to 37 kDa on SDS-PAGE, confirm the enzyme was homogenous, monomeric protein (Fig. 4). Reaction of purified APX with copper sulphate resulted in color change of reaction mixture from greenish blue to brownish green clearly indicate the formation of CuNPs. The spectrophotometric peaks at 547 nm and 638 nm in the visible region also support formation of CuNPs from cupper ions (Fig. 5a). The peak at 528 cm^{-1} in FTIR spectra is corresponds to the Cu-O bond also confirm the formation of CuNPs (Rahman, et al., 2013) (Fig. 5b). XRD measurements were carried out for the determination of crystal phase composition of titanium dioxide nanoparticles synthesized using plant extracts. The measurements were carried out over the diffraction angle (θ) 0–80° (Fig. 5c). Line broadening of the diffraction peaks indicates that the synthesized materials are in nanometer range. The diffraction pattern showed that
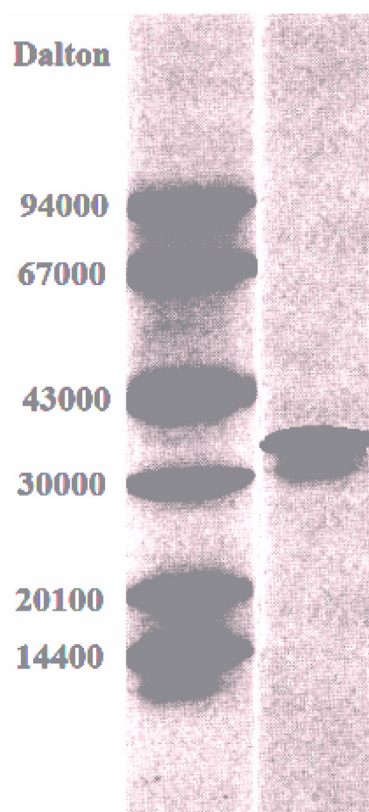
Fig. 4 SDS–PAGE of homogenous monomeric APX corresponding to 37 kDa purified from *S. polyrhiza* treated with 150 ppm NaCl + RV5 concentration.

nanoparticles synthesized using different plant extract were from anatase phase. As, the main peaks in the range of θ = 43.31°, matches the (1 0 1) crystallographic plane of anatase of CuNPs, indicating that nanoparticles structure dominantly correspond to anatase crystalline. The crystallite sizes of different synthesized nanoparticles were calculated using Scherrer equation (4) for the main peak,

$$d = 0.94\lambda/\beta Cos\theta \tag{4}$$

Table 2 Purification summary of APX isolated from *S. polyrhiza*.

Sr. No.	Step	Volume (ml)	Proteins (mg)	Activity (Unit)	Specific activity (Unit/mg)	Purification (fold)	Yield (%)
1	*S. polyrhiza*l extract	5000	98,500	22,310	0.226	1	100
2	DEAE-Sephadex	4123	61,784	20,870	0.338	1.49	93.55
3	CM-Sephadex	3367	49,214	18,740	0.381	1.68	84.00
4	Ammonium sulphate 55%	2135	32,980	17,950	0.544	2.40	80.46
5	DEAE-Sephadex	1654	28,760	16,990	0.591	2.61	76.15
6	G-200 Sephadex	1234	16,750	12,390	0.740	3.27	55.54
7	CM-Sephadex column	1109	12,780	10,940	0.856	3.78	49.04
8	G-200 Sephadex	1334	10,090	9430	0.935	4.13	42.27
9	Ammonium sulphate 35%	1045	7980	8900	1.115	4.92	39.89
10	Crystallization	976	6120	8800	1.438	6.35	39.44
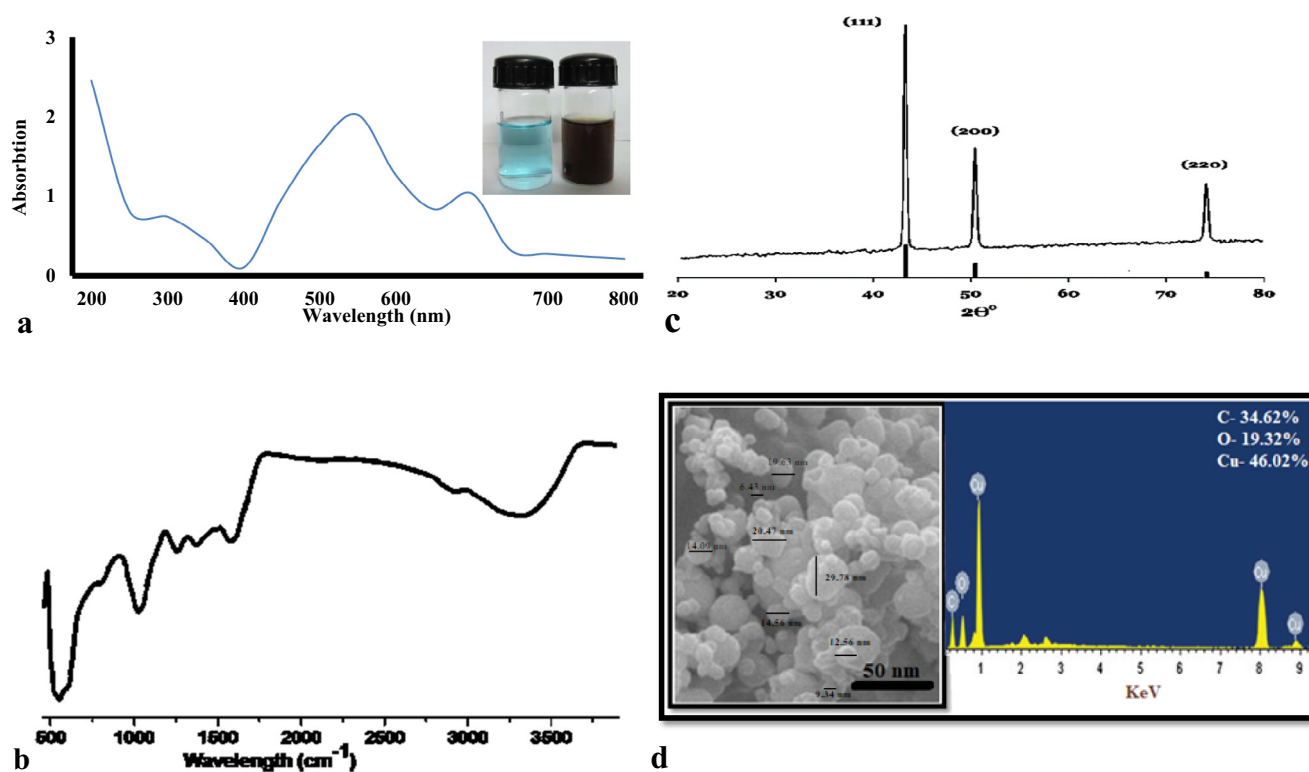
Fig. 5 Characterization of CuNPs, Uv–vis. Spectroscopic analysis (a), FTIR analysis (b), XRD graph (c) and SEM-EDXA analysis (d) synthesized by purified APX.

Where, d is the mean diameter of the nanoparticles, λ is wavelength of X-ray radiation source, β is the angular FWHM of the XRD peak at the diffraction angle θ.

Crystallite size of synthesized nanoparticles was found to be in the range of 11.08 to 98.69 nm. A very sharp intense peak at 43.31°, 50.44° and 74.12° 2θ in XRD graph were identified as 111, 200 and 220 (Fig. 4c) planes confirm the formation of zero-valent copper (Kamali et al 2020). Further, the size range of the CuNPs were 5–35 nm with an average size of ~23–26 nm were observed under SEM (Fig. 5d). The elemental Cu, C and Oxygen were observed in the SEM-EDX spectra of CuNPs.

3.4. Efficiency of CuNPs

As shown in Fig. 6a different reactive dyes were decolorized with varying the concentration from 100 to 1000 mg/l. The maximum degradation rate was 17.24 mg/L min. found for RV5 at 1000 mg/l after 1 h of incubation. However, the maximum rate of decolorization was 12.30, 11.56, 8.93 and 9.86 mg/L min achieved for RB222, RR31, RB-5 and RB220 respectively after 1.5 h incubation at 750 mg/L dye concentration, further increase in the concentration decrease % decolorization and the rate of decolorization (Fig. 6a). The present results revealed that the biogenic CuNPs possess excellent photocatalytic potential for the degradation of each dye up to 750 mg/L dye concentration. Significant increase in the degradation rate from 4.8 to 17.24 mg/L min was observed between 100 and 1000 mg/L concentration of RV5 dye, indicates potential of CuNPs for remediation of wide range of different reactive dyes. Various studies reported the role of

CuNPs in photocatalytic degradation of azo dyes (Sasikala et al., 2018). It also possesses excellent photocatalytic potential and decolorized 91.53%, 73.89% and 84.89% of the initial concentration of methylene blue, methyl red and Congo red respectively under solar irradiation (Fathima et al., 2018).

The stability of the CuNPs for complete decolorization was observed up to the 10th cycle with 250 mg/L RV5 with in 26 min. Afterward up to the 15th cycle the decolorization percentage was drastically fall up 40% with increase the incubation time up to 45 min. (Fig. 6b).

CuNPs were also tasted for the different RV5 concentrations in the experiment ranged from 50 to 25,000 mg/l. The results showed that the increasing the concentration of RV5 increased the rate of decolorization, COD and BOD reduction rate from 3.0 ± 0.19 to 80 ± 4.23 mg/L min., 2012.7 ± 407.61 to 55263.3 ± 3298.5 mg/m³min. and 899.25 ± 210.98 to 30560.3 ± 1987.5 mg/m³min. respectively (Fig. 6c). The maximum the rate of decolorization, COD and BOD reduction rate was achieved at 15,000 mg/l RV5 concentration, further increase in the concentration, decrease 18.06% rate of decolorization and 22.15% COD reduction rate and 17.66% BOD reduction rate. It might be due to the quantity of intermediates increased as well, competing through side reactions with the parent dye decomposition. It is suggested that the increased RV5 concentration resulted in increased capacity of the solution, thereby blocking more sun light from reaching the CuNPs, reduce the catalytic efficiency of CuNPs.

RV5 degradation products and intermediates were also analyzed, which resulted in a number of compounds that could be fitted to proposed degradation pathways. The predominant
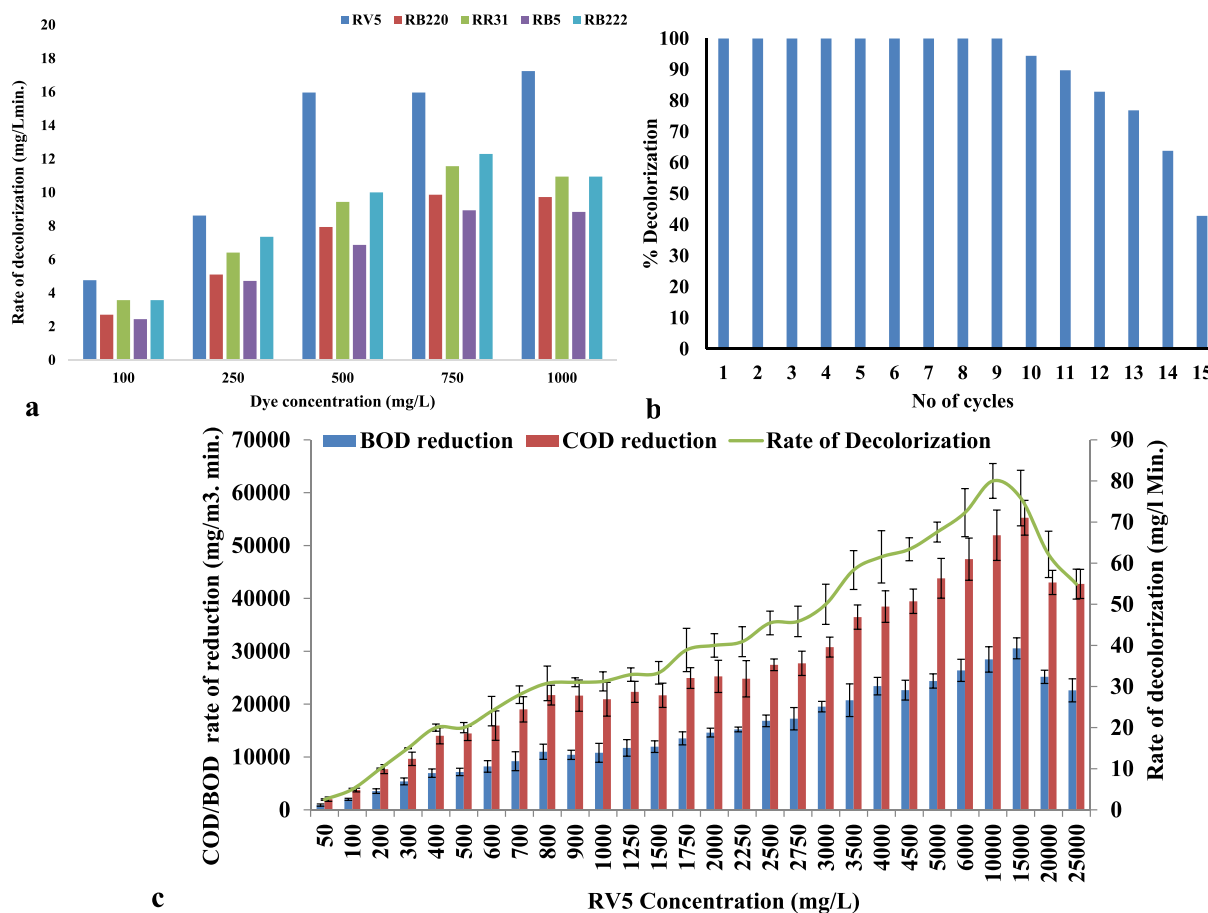
Fig. 6 Efficiency of CuNPs for; mineralization of wide spectrum of dyes (a), repetitive application of CuNPs for RV5 mineralization (b) effect of organic loading rate of RV5 on rate of decolorization, rate of COD and BOD reduction (c).

intermediate products formed in the photocatalytic degradation of RV5 in the solution during the initial phase of degradation were 6-amino naphthalene sulfonic acid, 4-amino benzenes sulfonic acid and unknown product. Subsequent increase in incubation time concentration of 2,4-Hepta-2,4-dienedioic acid, 2-Carboxy Benzoic acid, Trans o-hydroxy benzylidene pyruvate, 3-Pent-3-enoic acid and 3-[(3-Hydrazinophenyl)sulfonyl] propionic acid was clearly indicate (Fig. 7), broken the ring structure in to the lower molecular weight aliphatic hydrocarbons led to complete mineralization (Patel and Bhatt, 2015, Patel et al., 2020). Further it is clear that the degradation of some auxochrome/chromophore group which was only modifications phenyl ring configurations with the help of OH· random collision with RV5 and its intermediates products. Aliphatic acid intermediates readily might be converted into CO_2/H_2O or even smaller aliphatic hydrocarbons which cannot detected by the GC–MS analysis.

4. Conclusions

The present study comprehensively explored on cultivation of duckweed, green synthesis & degradation performances of CuNPs and bioethanol production in circular mechanism.
The following conclusions can be drawn from this work:

1. Nitrogen and phosphorus are major nutrients for the growth of duckweed, *S. polyrhiza* generate 3.25 ton of fresh biomass and reduce 89.5% TN and 96.7% TP of 1 MLD of sewage after 15 days of incubation.
2. NaCl combine with RV5 @150 ppm concentration was proven effective stress condition on *S. polyrhiza*, accumulate MAD (2.56 ± 0.1 nmol/mg protein), H_2O_2 (2.34 ± 0. 41 μmol/g FW), SOR (2.58 ± 0.57 μmol/g FW), SOD (345. 8 ± 61.64 Unit mg-1 protein), APX (741.8 ± 65.36 Unit mg^{-1} protein) and Starch (16.57 ± 2.35% of FW).
3. Production of bioethanol was 425.23 ± 2.84 mg/g reducing sugar achieved with 87.24 ± 1.24% conversion efficiency.
4. Purified APX was homogenous monomeric protein with 37 kDa MW and increase 6.35-fold specific enzyme activity after purification.
5. Average size of CuNPs synthesized by purified APX were observed 23–26 nm and rate of decolorization, COD and BOD reduction were 80 ± 4.23 mg/L min., 55263.3 ± 329 8.5 $mg/m^3min.$ and 30560.3 ± 1987.5 $mg/m^3min.$ achieved respectively.

In conclusion, this circular model will be a promising alternative for the treatment of wastewater containing organic micro-pollutants and energy generation.
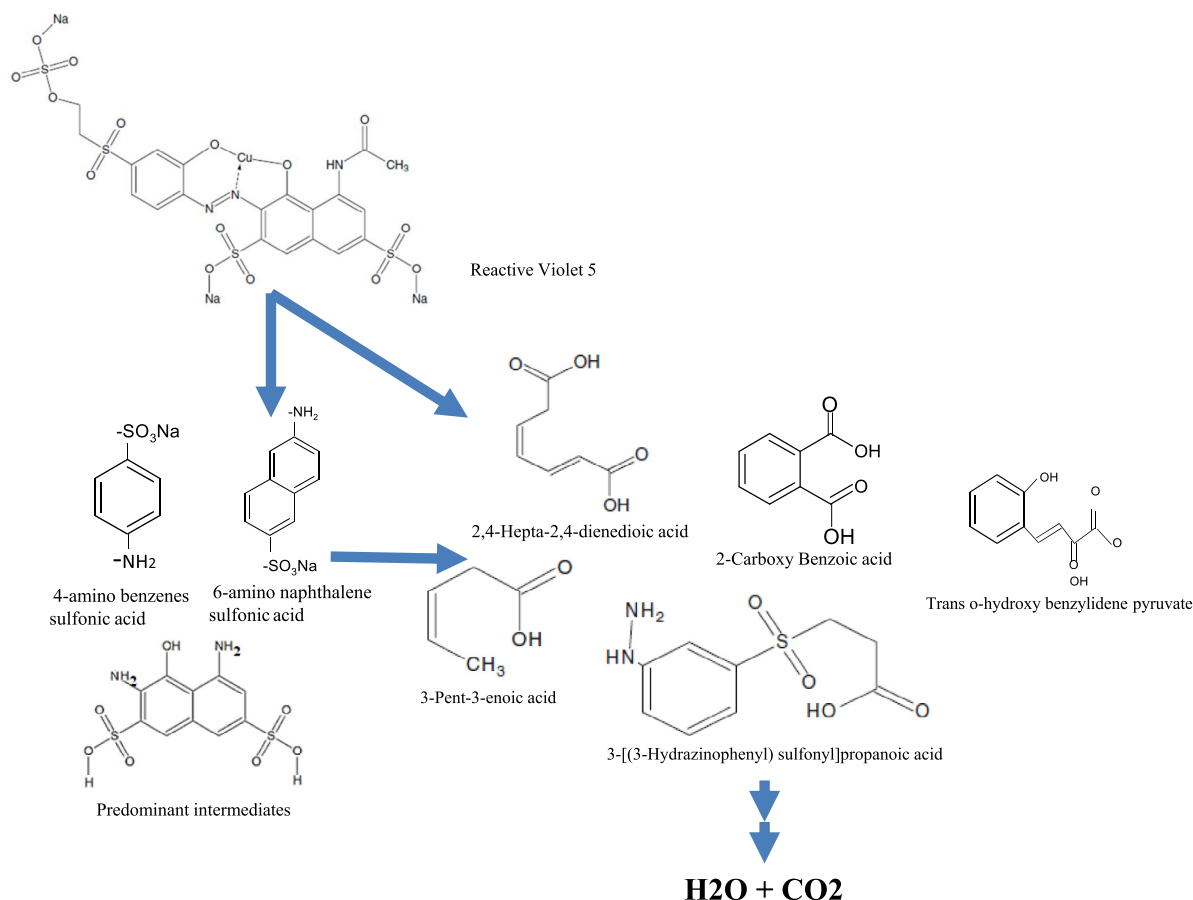
Fig. 7 Proposed mechanism for RV5 mineralization pathway.

Declaration of Competing Interest

The authors declare that they have no known competing financial interests or personal relationships that could have appeared to influence the work reported in this paper.

Appendix A. Supplementary material

Supplementary data to this article can be found online at https://doi.org/10.1016/j.arabjc.2020.10.008.

References

Abdelbasset, R., Issa, A.A., Adam, M.S., 1995. Chlorophyllase activity-effects of heavy metals and calcium.

Appenroth, K.J., Krech, K., Keresztes, A., Fischer, W., Koloczek, H., 2010. Effects of nickel on the chloroplasts of the duckweeds Spirodela polyrhiza and Lemna minor and their possible use in biomonitoring and phytoremediation. Chemosphere 78 (3), 216–223.

Ashraf, M., Harris, P.J.C., 2004. Potential biochemical indicators of salinity tolerance in plants. Plant Sci. 166, 3–16.

Beauchamp, C., Fridovich, I., 1971. Superoxide dismutase: improved assays and an assay applicable to acrylamide gels. Analy. Biochem. 44 (1), 276–287.

Belhaj, D., Frikha, D., Athmouni, K., Jerbi, B., Ahmed, M.B., Bouallagui, Z., Kallel, M., Maalej, S., Zhou, J., Ayadi, H., 2017. Box-Behnken design for extraction optimization of crude polysac-charides from Tunisian Phormidium versicolor cyanobacteria (NCC 466): partial characterization, in vitro antioxidant and antimicrobial activities. Int. J. Biol. Macromol. 105, 1501–1510.

Chaves, M.M., Flexas, J., Pinheiro, C., 2009. Photosynthesis under drought and salt stress: regulation mechanisms from whole plant to cell. Ann. Bot. 103, 551–560.

Chen, Q., Jin, Y.L., Zhang, G.H., Fang, Y., Xiao, Y., Zhao, H., 2012. Improving production of bioethanol from duckweed (Landoltia punctata) by pectinase pretreatment. Energies 5, 3019–3032.

Davis, B.J., 1964. Disc electrophoresis. II. Method and application to human serum proteins. Ann. NY Acad. Sci. 121 (2), 404–427.

Doğanlar, Z.B., Atmaca, M., 2011. Influence of airborne pollution on Cd, Zn, Pb, Cu, and Al accumulation and physiological parameters of plant leaves in Antakya (Turkey). Water, Air, Soil Pollut. 214 (1–4), 509–523.

Doke, N., 1983. Involvement of superoxide anion generation in the hypersensitive response of potato tuber tissues to infection with an incompatible race of Phytophthora infestans and to the hyphal wall components. Physiolog. Plant Pathol. 23 (3), 345–357.

Fathima, J.B., Pugazhendhi, A., Oves, M., Venis, R., 2018. Synthesis of eco-friendly copper nanoparticles for augmentation of catalytic degradation of organic dyes. J. Mol. Liquids 260, 1–8.

Geng, Q., Li, T., Li, P., Wang, X., Chu, W., Ma, Y., Ma, H., Ni, H., 2018. The accumulation, transformation, and effects of quinestrol in duckweed (Spirodela polyrhiza L.). Sci. Total Environ. 634, 1034–1041.

Gill, S.S., Tuteja, N., 2010. Reactive oxygen species and antioxidant machinery in abiotic stress tolerance in crop plants. Plant Physiol. Biochem. 48 (12), 909–930.

Guo, L., Ding, Y., Xu, Y., Li, Z., Jin, Y., He, K., Fang, Y., Zhao, H., 2017. Responses of Landoltia punctata to cobalt and nickel: Removal, growth, photosynthesis, antioxidant system and starch metabolism. Aquatic Toxic. 190, 87–93.

Kamali, M., Davarazar, M., Aminabhavi, T.M., 2020. Single precursor sonochemical synthesis of mesoporous hexagonal-shape zerovalent copper for effective nitrate reduction. Chem. Eng. J. 384, 123359.

Mishra, S., Srivastava, S., Tripathi, R.D., Kumar, R., Seth, C.S., Gupta, D.K., 2006. Lead detoxification by coontail (Ceratophyllum demersum L.) involves induction of phytochelatins and antioxidant system in response to its accumulation. Chemosphere 65 (6), 1027–1039.

Nakano, Y., Asada, K., 1981. Hydrogen peroxide is scavenged by ascorbate specific peroxidase in spinach chloroplasts. Plant. Cell Physiol. 22, 867–880.

Patel, V.R., Bhatt, N., 2015. Isolation, development and identification of salt-tolerant bacterial consortium from crude-oil-contaminated soil for degradation of di-azo dye Reactive Blue 220. Water Sci. Tech. 72 (2), 311–321.

Patel, V.R., Bhatt, N.S., Bbhatt, H., 2013. Involvement of ligninolytic enzymes of Myceliophthora vellerea HQ871747 in decolorization and complete mineralization of Reactive Blue 220. Chem. Eng. J. 233, 98–108.

Patel, V.R., Khan, R., Bhatt, N., 2020. Cost-effective in-situ remediation technologies for complete mineralization of dyes contaminated soils. Chemosphere 243, 125253.

Potters, G., Horemans, N., Jansen, M.A.K., 2010. The cellular state in plant stress biology – a charging concept. Plant Physiol. Biochem. 48, 292–300.

Rajkumar, R., Yaakob, Z., Takriff, M.S., 2014. Potential of micro and macro algae for biofuel production: a brief review. Bioresources 9 (1), 1606–1633.

Rahman, M.M., Khan, S.B., Gruner, G., Al-Ghamdi, M.S., Daous, M.A., Asiri, A.M., 2013. Chloride ion sensors based on low-dimensional α-MnO2–Co3O4 nanoparticles fabricated glassy carbon electrodes by simple I-V technique. Electrochim. Acta 103, 143–150.

Ruiz-Lozano, J.M., Aroca, R., 2010. In: Modulation of Aquaporin Genes by the Arbuscular Mycorrhizal Symbiosis in Relation to Osmotic Stress Tolerance. Springer, Dordrecht, pp. 357–374.

Singh, R., Shedbalkar, U.U., Nadhe, S.B., Wadhwani, S.A., Chopade, B.A., 2017. Lignin peroxidase mediated silver nanoparticle synthesis in Acinetobacter sp. AMB Express 7 (1), 226.

Singh, V., Pandey, B., Suthar, S., 2018. Phytotoxicity of amoxicillin to the duckweed Spirodela polyrhiza: growth, oxidative stress, biochemical traits and antibiotic degradation. Chemosphere 201, 492–502.

Singh, V.K., Singh, J., 2006. Toxicity of industrial wastewater to the aquatic plant Lemna minor L. J. Environ. Bio. 37 (2), 385–390.

Sree, K.S., Appenroth, K.J., 2014. Increase of starch accumulation in the duckweed Lemna minor under abiotic stress. Albanian J. Agri. Sci., 11

Sumithra, K., Jutur, P.P., Carmel, B.D., Reddy, A.R., 2006. Salinity-induced changes in two cultivars of Vigna radiata: responses of antioxidative and proline metabolism. Plant Growth Regul. 50, 11–22.

Sundar, S., Venkatachalam, G., Kwon, S.J., 2018. Biosynthesis of copper oxide (CuO) nanowires and their use for the electrochemical sensing of dopamine. Nanomaterials 8 (10), 823.

Torbati, S., Movafeghi, A., Khataee, A.R., 2015. Biodegradation of CI Acid Blue 92 by Nasturtium officinale: study of some physiological responses and metabolic fate of dye. Internat. J. Phytoremed. 17 (4), 322–329.

Verma, R., Suthar, S., 2014. Synchronized urban wastewater treatment and biomass production using duckweed Lemna gibba L. Ecol. Eng. 64, 337–343.

WWAP (United Nations World Water Assessment Programme), UNESCO, 2017.

Xu, J., Cui, W., Cheng, J.J., Stomp, A.M., 2011. Production of high-starch duckweed and its conversion to bioethanol. Biosys. Eng. 110 (2), 67–72.

Yamaya, T., Matsumoto, H., 1989. Accumulation of asparagines in NaCl-stressed barley seedlings. Berichte des Ohara Institut fur Landwirtschaftliche Biologie, Okayama Universitat 19, 181–188.